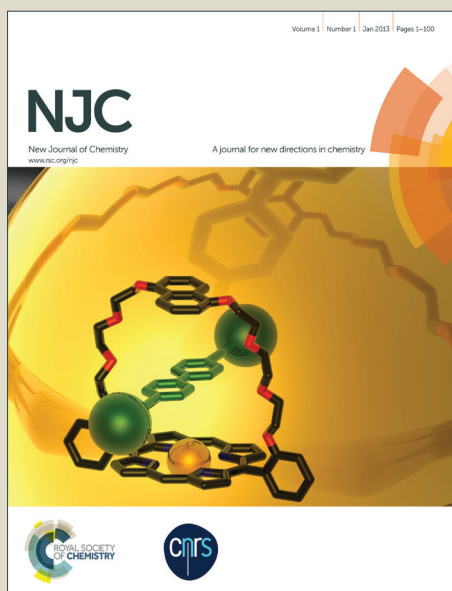


NJC

Accepted Manuscript



This is an *Accepted Manuscript*, which has been through the Royal Society of Chemistry peer review process and has been accepted for publication.

Accepted Manuscripts are published online shortly after acceptance, before technical editing, formatting and proof reading. Using this free service, authors can make their results available to the community, in citable form, before we publish the edited article. We will replace this *Accepted Manuscript* with the edited and formatted *Advance Article* as soon as it is available.

You can find more information about *Accepted Manuscripts* in the [Information for Authors](#).

Please note that technical editing may introduce minor changes to the text and/or graphics, which may alter content. The journal's standard [Terms & Conditions](#) and the [Ethical guidelines](#) still apply. In no event shall the Royal Society of Chemistry be held responsible for any errors or omissions in this *Accepted Manuscript* or any consequences arising from the use of any information it contains.

Synthesis, characterization and anticancer activity of dinuclear ruthenium(II) complexes linked by alkyl chain

Yan Zhang ^a, Lu Lai ^b, Ping Cai ^{a*}, Gong-Zhen Cheng ^{a*}, Yi Liu ^a

Received (in XXX, XXX) Xth XXXXXXXXXX 20XX, Accepted Xth XXXXXXXXXX 20XX

DOI: 10.1039/b000000x

A series of 1,10-phenanthroline-based dinucleating bridging ligands **BL**¹⁻³ and their dinuclear Ru(II) complexes [(bpy)₂Ru(BL¹⁻³)Ru(bpy)₂](PF₆)₄ (bpy = 2,2'-bipyridine) have been synthesized and characterized by elemental analysis, IR, NMR and mass spectrometry methods. Their photophysical and electrochemical properties have been studied. The symmetric nature of the bridging ligands enabled the formation of dinuclear Ru(II) complexes **1-3** with equivalent metal centers. The complexes **1-3** exhibited the spin-allowed ¹MLCT (*d*_π-π*) transition at approximate 460 nm and Ru(II) metal centered emission at around 600 nm in solution at room temperature. The emission profile and emission maxima are similar and independent of the excitation wavelength for each complex. The complexes **1-3** undergo metal centered oxidation and the *E*_{1/2} values for the Ru(II)/Ru(III) redox couple are 0.9 and 1.4 V versus *SCE*. The cytotoxicity of these complexes in vitro was evaluated by MTT (3-(4, 5-dimethylthiazol-2-yl)-2, 5-diphenyltetrazolium bromide) assay. The result indicated that the Ru(II) complexes **1-3** exhibited significant dose-dependent cytotoxicity to cervical cancer(Hela), gastric cancer(SGC-7901) and gastric cancer (BGC823) tumour cell lines. It is worth noting that the cytotoxicity of the complexes **1-3** increased with the increase of methylene of bridging ligands. The DNA-quenching constants were determined to be 1.34×10⁵, 1.46×10⁵ and 2.98×10⁵ mol⁻¹ L for **1**, **2** and **3**, respectively, indicating that the different interactions between complexes **1-3** with DNA.¹

a: College of Chemistry and Molecular Sciences, Wuhan University, Wuhan, 430072, China E-mail: caiping@whu.edu.cn

b: College of Chemistry and Environmental Engineering, Yangtze University, Jingzhou, 434023, China

1. Introduction

Ruthenium complexes as antitumor agents are very promising in the field of non-platinum complexes showing activity in tumors which developed resistance to cisplatin (*cis*-[PtCl₂(NH₃)₂]) or in which cisplatin is inactive.¹⁻⁵ Up to now, a large number of ruthenium complexes have been synthesized and tested for therapeutic potential.⁶⁻¹¹ For example, two Ru(III) complexes have entered clinical trials: KP1019 and NAMI-A.¹²⁻¹³ The design and construction of new ruthenium complexes have been the subject of considerable attention by many research groups over the past decade. In particular, much attention is devoted to 2,2'-bipyridine (bpy) due to its high complexing affinity with a variety of metal ions and interesting photophysical, photochemical, and electron transfer properties of its metal complexes.¹⁴ Ru(II) complexes of polypyridine ligands,¹⁵ because of their unique combination of chemical stability, redox properties, luminescence intensity and cytotoxicity, have been used extensively to construct supramolecular systems.¹⁶ Since the luminescence, redox behavior and cytotoxicity of Ru(II) complexes are strongly ligand-dependent, considerable research interest has been dedicated to fine-tune these properties by changing the commonly employed polypyridyl ligands.¹⁷ The convenient features of pyridine as a coordinating molecule was introduced in various bridging

ligands to assemble dinuclear and polynuclear supramolecular.¹⁸ The shape, size and functions of these complexes depend to a large extent on the nature of the bridging ligands which connect the metal centers. The crucial role played by bridging ligands in determining the ground state metal-metal interaction is well recognized.¹⁹ The flexibly linked species show an enhanced affinity as torsional rotation and allow the second metal center to position and bind (although less strongly) in the minor groove at a duplex region adjacent to the non-duplex feature, rather than being extra-helical as is the case in the rigidly-linked species. Here, we reported a series of new phenanthroline-based flexible dinucleating bridging ligands (**BL**¹⁻³) and their dinuclear Ru(II) complexes **1-3** with 2,2'-bipyridine as ancillary ligands. The cytotoxicity in vitro of the complexes was evaluated by MTT assay and the interaction of Ruthenium(II) complexes with DNA was studied by electronic emission titration.

2. Experimental

2.1 Materials and instrumentation

All reagents and solvents were of commercial origin and were used without further purification unless otherwise noted. Ultrapure Milli-Q water was used in all experiments. Dimethyl sulfoxide (DMSO) and RPMI 1640 were purchased from Sigma. Hela (human cervical carcinoma), BGC823 (Human gastric carcinoma) and SGC-7901 (Human gastric carcinoma) cell lines

were purchased from the American Type Culture Collection. RuCl₃·3H₂O, 2,2'-bipyridyl (bpy), 5-amino-1,10-phenanthroline, 1,2-ethyl bromide, 1,3-dibromopropane, 1,4-dibromobutane, 4-hydroxybenzaldehyde were purchased from the Wu han Shen shi Hua gong, Ru(bpy)₂Cl₂·2H₂O (bpy = 2,2'-bipyridyl) was synthesized and purified according to the literature methods.²⁰ Microanalysis (C, H, O and N) were conducted with a PerkinElmer 240Q Elemental Analyzer. Electrospray Ionization Mass Spectra were recorded with an LCQ system (Finnigan MAT, USA) using CH₃OH as the mobile phase. 300 MHz ¹H NMR spectroscopic measurements were performed on a Bruker AM-300 NMR spectrometer, using CDCl₃ and d₆-DMSO as solvent and TMS (SiMe₄) as an internal reference at 25°C. Infrared spectra were recorded on a Perkin-Elmer Spectrum FT-IR Spectrometer using KBr pellets. Solution electronic absorption spectra and emission spectra in acetonitrile were recorded on Shimadzu 3100 spectrophotometer and Shimadzu RF-5301 PC spectrofluorometer, respectively. Cyclic voltammetry (CV) were obtained with CHI 630E instrument in a three-electrode cell with a pure Ar gas inlet and outlet. The working electrode and counter electrode were Pt electrode, and the reference electrode was a saturated calomel electrode (SCE). The experiments were carried out in the presence of CH₃CN and scan rate was 100 mV·s⁻¹.

2.2 Synthesis

2.2.1 Synthesis of the bridging ligands BL¹⁻³

Stage-1: Synthesis of dialdehyde

The dialdehyde were synthesized according to the method reported by Donahoe *et al.*²¹ A solution of sodium hydroxide (8 g, 200 mmol) in water (40 mL) was added to a solution of 4-hydroxybenzaldehyde (24.4 g, 200 mmol) in ethanol (40 mL), warmed, and then 1,2-dibromoalkane (100 mmol) was added followed by ethanol (40 mL) to get a homogeneous solution. The solution was refluxed under nitrogen atmosphere for 20 h, cooled to 0 °C, and the colorless needles that separated out was filtered, washed with water, and recrystallized in ethanol.

4,4'-(ethane-1,2-diylbis(oxy))dibenzaldehyde:

C₁₆H₁₄O₄ (0.25 g, 92 %). Anal. Calc: C, 71.11; H, 5.18; O, 23.71. Found: C, 71.08; H, 5.21; O, 23.66%. ¹H NMR(300 MHz; CDCl₃; 298 K): 4.45 (s, 4H, -O-CH₂), 7.06 (d, 4H, J=6.0 Hz, Ph), 7.86 (d, 4H, J=6.0 Hz, Ph), 9.91 (s, 2H, -CHO).

4,4'-(propane-1,3-diylbis(oxy))dibenzaldehyde:

C₁₇H₁₆O₄ (0.24 g, 85 %). Anal. Calc: C, 71.83; H, 5.63; O, 22.54. Found: C, 71.85; H, 5.61; O, 22.60%. ¹H NMR(300 MHz; CDCl₃; 298 K): 2.35(m, 2H, -CH₂), 4.27 (m, 4H, -O-CH₂), 7.01 (d, 4H, J=9.0 Hz, Ph), 7.83 (d, 4H, J=9.0 Hz, Ph), 9.89 (s, 2H, -CHO).

4,4'-(butane-1,4-diylbis(oxy))dibenzaldehyde:

C₁₈H₁₈O₄ (0.27 g, 90 %). Anal. Calc: C, 72.48; H, 6.04; O, 21.48. Found: C, 72.45; H, 6.07; O, 21.51%. ¹H NMR(300 MHz; CDCl₃; 298 K):

2.05(s, 4H, -CH₂), 4.14 (s, 4H, -O-CH₂), 6.99 (d, 4H, J=9.0 Hz, Ph), 7.83 (d, 4H, J=9.0 Hz, Ph), 9.89 (s, 2H, -CHO).

Stage-2: Synthesis of Schiff base L^{1-3}

To a solution of 5-amino-1,10-phenanthroline (0.39 g, 2 mmol) was added a solution of dialdehyde (1 mmol) in methanol (10 mL), glacial acetic acid was added dropwise with stirring in nitrogen atmosphere, refluxed for 5 h, cooled to room temperature, a pale yellow precipitate separated out. The product was filtered, washed with large portions of ethanol, and dried in vacuo.

L^1 : C₄₀H₂₈N₆O₂ (0.47 g, 75 %). Anal. Calc: C, 76.92; H, 4.49; N, 13.46. Found: C, 76.88; H, 4.45; N, 13.41%. IR (cm⁻¹, KBr): 2936(C-H), 1598 (C=N), 1423 (C=C), 1230 (C-O-C), 1062 (C-O-C), 801 (C-H) (pyridine), 734(β-ring) (pyridine), 617(C-C). ¹H NMR(300 MHz; CDCl₃; 298 K): 4.50 (s, 4H, -O-CH₂), 7.12 (d, 4H, J=9.0 Hz, H₁₂), 7.30 (s, 2H, H₆), 7.59-7.68 (m, 4H, H₃, H₈), 8.02 (d, 4H, J = 9.0 Hz, H₁₁), 8.21 (d, 2H, J = 6.0 Hz, H₇), 8.64 (s, 2H, H₁₀), 8.78 (d, 2H, J = 6.0 Hz, H₄), 9.12 (d, 2H, J = 3.0 Hz, H₉), 9.23 (d, 2H, J = 3.0 Hz, H₂).

L^2 : C₄₁H₃₀N₆O₂ (0.46 g, 72 %). Anal. Calc: C, 77.12; H, 4.70; N, 13.17. Found: C, 77.15; H, 4.69; N, 13.16%. IR (cm⁻¹, KBr): 2935(C-H), 1601(C=N), 1420(C=C), 1228 (C-O-C), 1060 (C-O-C), 805 (C-H) (pyridine), 735(β-ring) (pyridine), 615(C-C). ¹H NMR(300 MHz; CDCl₃; 298 K): 2.38(t, 2H, -CH₂), 4.31 (t, 4H, -O-CH₂), 7.08 (d, 4H, J=9.0 Hz, H₁₂), 7.28 (s, 2H, H₆),

7.58-7.67 (m, 4H, H₃, H₈), 7.99 (d, 4H, J = 9.0 Hz, H₁₁), 8.19 (d, 2H, J = 9.0 Hz, H₇), 8.62 (s, 2H, H₁₀), 8.76 (d, 2H, J = 9.0 Hz, H₄), 9.11 (d, 2H, J = 3.0 Hz, H₉), 9.22 (d, 2H, J = 3.0 Hz, H₂). L^3 : C₄₂H₃₂N₆O₂ (0.41 g, 63 %). Anal. Calc: C, 77.30; H, 4.91; N, 12.88. Found: C, 77.28; H, 4.90; N, 12.91%. IR (cm⁻¹, KBr): 2930(C-H), 1599(C=N), 1418(C=C), 1226 (C-O-C), 1061 (C-O-C), 802 (C-H) (pyridine), 731(β-ring) (pyridine), 614(C-C). ¹H NMR(300 MHz; CDCl₃; 298 K): 2.10(s, 4H, -CH₂), 4.19 (s, 4H, -O-CH₂), 7.05 (d, 4H, J=9.0 Hz, H₁₂), 7.29 (s, 2H, H₆), 7.56-7.65 (m, 4H, H₃, H₈), 7.99 (d, 4H, J = 9.0 Hz, H₁₁), 8.20 (d, 2H, J = 6.0 Hz, H₇), 8.62 (s, 2H, H₁₀), 8.77 (d, 2H, J = 9.0 Hz, H₄), 9.11 (d, 2H, J = 3.0 Hz, H₉), 9.22 (d, 2H, J = 3.0 Hz, H₂).

Stage-3: Synthesis of bridging ligands BL^{1-3}

To a solution of L^{1-3} (1 mmol) in ethanol (40 mL) was added a solution of sodium borohydride (0.076 g, 2 mmol) in ethanol (10 mL). The solution was refluxed under nitrogen atmosphere for 4 h, cooled to room temperature, a pale yellow precipitate separated out. The product was filtered, washed with large portions of ethanol and dried in vacuo.

BL^1 : C₄₀H₃₂N₆O₂ (0.37 g, 59 %). Anal. Calc: C, 76.43; H, 5.09; N, 13.38. Found: C, 76.42; H, 5.11; N, 13.32%. IR (cm⁻¹, KBr): 3321(N-H), 2936(C-H), 1599(C=C), 1498 (C=C), 1229(C-N), 1045(C-O-C), 818(C-H) (pyridine), 734(β-ring) (pyridine), 624(C-C). ¹H NMR(300 MHz; CDCl₃; 298K): 4.37 (s, 4H, -O-CH₂), 4.52(s, 4H, -N-CH₂), 4.71(s, 2H, -NH), 6.75(s, 2H, H₆), 6.99

(d, 4H, J=9.0 Hz, H₁₃), 7.41 (d, 4H, J=9.0 Hz, H₁₂), 7.47-7.51 (m, 2H, H₃), 7.61-7.65(m, 2H, H₈), 7.99 (d, 2H, J = 6.0 Hz, H₄), 8.27 (d, 2H, J = 9.0 Hz, H₇), 8.90 (d, 2H, J = 3.0 Hz, H₂), 9.19 (d, 2H, J = 3.0 Hz, H₉).

BL²: C₄₁H₃₄N₆O₂ (0.41 g, 64 %). Anal. Calc: C, 76.64; H, 5.29; N, 13.08. Found: C, 76.71; H, 5.31; N, 13.06%. IR (cm⁻¹, KBr): 3285(N-H), 2936(C-H), 1607(C=C), 1500(C=C), 1327(C-N), 1046 (C-O-C), 823(C-H) (pyridine), 736(β-ring) (pyridine), 622(C-C). ¹H NMR(300 MHz; CDCl₃; 298K): 2.29(m, 2H, -CH₂), 4.21 (m, 4H, -O-CH₂), 4.49(s, 4H, -N-CH₂), 4.70 (s, 2H, -NH), 6.75(s, 2H, H₆), 6.95 (d, 4H, J=9.0 Hz, H₁₃), 7.39 (d, 4H, J=9.0 Hz, H₁₂), 7.47-7.51 (m, 2H, H₃), 7.60-7.64(m, 2H, H₈), 7.99 (d, 2H, J = 9.0 Hz, H₄), 8.26 (d, 2H, J = 9.0 Hz, H₇), 8.89 (d, 2H, J = 3.0 Hz, H₂), 9.18 (d, 2H, J = 3.0 Hz, H₉).

BL³: C₄₂H₃₆N₆O₂ (0.39 g, 59 %). Anal. Calc: C, 76.83; H, 5.49; N, 12.80. Found: C, 76.85; H, 5.44; N, 12.90%. IR (cm⁻¹, KBr): 3329(N-H), 2936(C-H), 1593(C=C), 1500(C=C), 1291(C-N), 1032 (C-O-C), 816(C-H) (pyridine), 729(β-ring) (pyridine), 622(C-C). ¹H NMR(300 MHz; CDCl₃; 298K): 2.03(s, 4H, -CH₂), 4.08 (s, 4H, -O-CH₂), 4.50(s, 4H, -N-CH₂), 4.64 (s, 2H, -NH), 6.77(s, 2H, H₆), 6.94 (d, 4H, J=9.0 Hz, H₁₃), 7.40 (d, 4H, J=9.0 Hz, H₁₂), 7.50-7.54 (m, 2H, H₃), 7.60-7.64(m, 2H, H₈), 8.00 (d, 2H, J = 6.0 Hz, H₄), 8.26 (d, 2H, J = 9.0 Hz, H₇), 8.91 (d, 2H, J = 3.0 Hz, H₂), 9.19 (d, 2H, J = 3.0 Hz, H₉).

2.2.2 Synthesis of dinuclear Ruthenium complexes 1-3

AgNO₃(0.17 g, 1.0 mmol) was added to an ethanol solution of Ru(bpy)₂Cl₂ · 2H₂O (0.26 g, 0.5 mmol). After refluxing for 30 min and filtering to remove the deposited AgCl, the filtrate was added to an ethanol solution of **BL¹⁻³**(0.25 mmol). The mixture was refluxed under the protection of nitrogen atmosphere for 24 h. After most of the solvent was removed under a reduced pressure, an orange-red precipitate was obtained by the dropwise addition of a 4-fold excess of saturated aqueous KPF₆ solution. The purification was carried out by column chromatography on neutral aluminium oxide with CH₃CN-H₂O-saturated aqueous KNO₃ (10:3:1, v/v/v) as eluent followed by reprecipitation with a saturated KPF₆ aqueous solution. Orange-red powder was obtained in >60% yields.

[Ru(bpy)₂-BL¹-Ru(bpy)₂](PF₆)₄, complex 1: Yield: 65%. Anal. Calcd for C₈₀H₆₄N₁₄O₂Ru₂(PF₆)₄: C, 47.20; H, 3.15; N, 9.64. Found: C, 47.26; H, 3.14; N, 9.66. IR (cm⁻¹, KBr): 3329(N-H), 2936(C-H), 1593(C=C), 1500(C=C), 1291(C-N), 1032 (C-O-C), 816(C-H) (pyridine), 729(β-ring) (pyridine), 622(C-C). ¹H NMR (300 MHz; DMSO-*d*₆; 298K): 4.00(s, 2H, -NH), 4.26 (s, 4H, -O-CH₂), 4.57(s, 4H, -N-CH₂), 6.87(s, 2H, H₆), 6.94 (d, 4H, J=6.0 Hz, H₁₃), 7.27 (d, 4H, J=9.0 Hz, H₁₂), 7.37-7.44 (m, 4H, H₃, H₈), 7.77-7.82(m, 12H, bpy), 7.95 (d, 2H, J = 9.0 Hz, H₄), 8.08(m, 4H, bpy), 8.15(m, 4H, bpy), 8.19(d, 4H, J = 9.0 Hz, bpy), 8.26 (d, 2H, J = 9.0 Hz, H₇), 8.27(m, 4H, bpy), 8.81 (d, 2H, J = 3.0 Hz,

H₂), 8.84(m, 4H, bpy), 9.05(d, 2H, J = 3.0 Hz, H₉). UV-vis in CH₃CN: λ/nm ($\epsilon/10^5 \text{ dm}^3 \text{ mol}^{-1} \cdot \text{cm}^{-1}$): 286 (1.42); 362 (0.23); 460 (0.26). ESI-MS: m/z 363.7 [M-4PF₆]⁴⁺ (calcd: 363.5)

[Ru(bpy)₂-BL²-Ru(bpy)₂](PF₆)₄, complex 2:
Yield: 60%. Anal. Calcd for C₈₁H₆₆N₁₄O₂Ru₂(PF₆)₄: C, 47.46; H, 3.22; N, 9.57. Found: C, 47.44; H, 3.18; N, 9.56. IR (cm⁻¹, KBr): 3325(N-H), 2930(C-H), 1579(C=C), 1495(C=C), 1237(C-N), 1032 (C-O-C), 835(C-H) (pyridine), 781(β -ring) (pyridine), 637(C-C). ¹H NMR (300 MHz; DMSO-*d*₆; 298K): 2.13(m, 2H, -CH₂), 4.01(s, 2H, -NH), 4.07 (m, 4H, -O-CH₂), 4.56(s, 4H, -N-CH₂), 6.89(s, 2H, H₆), 6.94 (d, 4H, J=6.0 Hz, H₁₃), 7.39 (d, 4H, J=9.0 Hz, H₁₂), 7.42-7.51 (m, 4H, H₃, H₈), 7.79-7.84(m, 12H, bpy), 7.97 (d, 2H, J = 9.0 Hz, H₄), 8.09(m, 4H, bpy), 8.15(m, 4H, bpy), 8.19(d, 4H, J = 9.0 Hz, bpy), 8.26 (d, 2H, J = 9.0 Hz, H₇), 8.27(m, 4H, bpy), 8.81 (d, 2H, J = 3.0 Hz, H₂), 8.84(m, 4H, bpy), 9.07(d, 2H, J = 3.0 Hz, H₉). UV-vis in CH₃CN: λ/nm ($\epsilon/10^5 \text{ dm}^3 \text{ mol}^{-1} \text{ cm}^{-1}$): 286(1.33); 360(0.23); 461(0.23). ESI-MS: m/z 367.2 [M-4PF₆]⁴⁺ (calcd: 367.0)

[Ru(bpy)₂-BL³-Ru(bpy)₂](PF₆)₄, complex 3:
Yield: 62%. Anal. Calcd for C₈₂H₆₈N₁₄O₂Ru₂(PF₆)₄: C, 47.72; H, 3.30; N, 9.51. Found: C, 47.70; H, 3.28; N, 9.46. IR (cm⁻¹, KBr): 3415(N-H), 2939(C-H), 1600(C=C), 1507(C=C), 1377(C-N), 1025 (C-O-C), 758(C-H) (pyridine), 722(β -ring) (pyridine), 657(C-C). ¹H NMR (300 MHz; DMSO-*d*₆; 298K): 1.83(s, 4H, -CH₂), 3.99

(s, 4H, -O-CH₂), 4.00(s, 2H, -NH), 4.56(s, 4H, -N-CH₂), 6.89(s, 2H, H₆), 6.92 (d, 4H, J=6.0 Hz, H₁₃), 7.16-7.24 (m, 4H, H₃, H₈), 7.42 (d, 4H, J=9.0 Hz, H₁₂), 7.57-7.59 (m, 12H, bpy), 7.83 (d, 2H, J = 9.0 Hz, H₄), 8.08(m, 4H, bpy), 8.13(m, 4H, bpy), 8.19(d, 4H, J = 9.0 Hz, bpy), 8.26 (d, 2H, J = 9.0 Hz, H₇), 8.27(m, 4H, bpy), 8.67 (d, 2H, J = 3.0 Hz, H₂), 8.82(m, 4H, bpy), 9.05(d, 2H, J = 9.0 Hz, H₉). UV-vis in CH₃CN: λ/nm ($\epsilon/10^5 \text{ dm}^3 \text{ mol}^{-1} \text{ cm}^{-1}$): 286 (2.41); 353 (0.41); 464 (0.45). ESI-MS: m/z 371.2 [M-4PF₆]⁴⁺ (calcd: 370.5), 542.8[M-3PF₆]³⁺ (calcd: 542.3), 887.2[M-2PF₆]²⁺ (calcd: 886.0).

2.3 Methods

2.3.1 MTT assays

Standard MTT(3-(4, 5-dimethylthiazol-2-yl)-2, 5-diphenyltetrazolium bromide) assay procedures were used.²² Cells were placed in 96-well microassay culture plates (8×10³ cells per well) and grown overnight at 37 °C in a 5% CO₂ incubator. The complexes tested were then added to the wells to achieve final concentrations ranging from 0.39×10⁻⁶ to 10⁻⁴ $\mu\text{mol L}^{-1}$. Control wells were prepared by addition of culture medium (200 μL). The plates were incubated at 37 °C in a 5% CO₂ incubator for 48 h. On completion of the incubation, stock MTT dye solution (20 μL , 5 mg mL⁻¹) was added to each well. After 4 h, 150 μL dimethylsulfoxide (DMSO) was added to solubilize the MTT formazan. The optical density of each well was then measured with a microplate spectrophotometer at a wavelength of 490 nm.

The IC₅₀ values were determined by plotting the percentage viability versus the concentration and reading off the concentration at which 50 % of the cells remained viable relative to the control.

Each experiment was repeated at least three times to obtain the mean values. Three different tumor cell lines were the subjects of this study: Hela (human cervical carcinoma), BGC823 (human gastric carcinoma), and SGC-7901 (human gastric carcinoma).

2.3.2 Fluorescence spectra

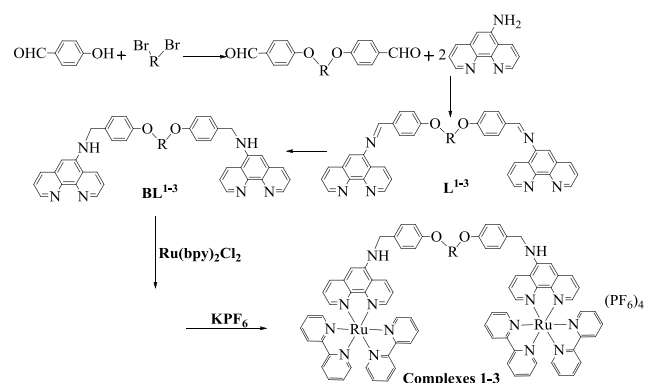
Fluorescence measurements were carried out by keeping the concentration of complexes constant (10 μM) and varying the concentration of CT-DNA from 20 to 100 μM. The complexes were excited at 465 nm and the fluorescence spectra were recorded between 500 and 800 nm.

3. Results and discussion

3.1 ¹H NMR of the bridging ligands BL¹⁻³

The synthetic route of the bridging ligands BL¹⁻³ and the complexes 1-3 was depicted in Scheme 1. The precursors dialdehyde were synthesized by modifying the procedure reported by Donahoe *et al.*²¹ (¹H NMR of dialdehyde in Supporting Information Fig.1). The Schiff bases L¹⁻³ were obtained as yellow powder by reacting the dialdehyde and 5-amino-1,10-phenanthroline in the presence of glacial acetic acid in methanol. The L¹⁻³ gave satisfactory elemental analysis, the IR spectra of all the three ligands shown the presence of any band around 1600 cm⁻¹, which indicated the formation of C=N in the Schiff base, and the ¹H NMR spectra of L¹⁻³ were recorded in

CDCl₃. The ¹H NMR spectrum of L¹ shown ten sets of signals in the aromatic region, as illustrated in Supporting Information Fig. 2. The signal assignment was rather straightforward by the comparison of chemical shifts with those of similar Schiff-base ligands, the resonances at 9.23, 9.12, 8.78, 8.21, 7.65, 7.59 and 7.27 ppm were assigned to the H₂, H₉, H₄, H₇, H₃, H₈ and H₆ protons, respectively, of the phenanthroline ring. The resonances at 8.02 and 7.12 ppm were assigned to the H₁₁ and H₁₂ protons, respectively, of the phenyl spacer. The H₁₃ (methylene) protons of the linker moiety resonated at 4.47 ppm. It's worth noting that there was a singlet at 8.64 ppm, which indicated formation of -C=N in the Schiff base. The bridging ligands BL¹⁻³ were synthesized by reducing the L¹⁻³ in the presence of sodium borohydride.



Scheme 1 Synthetic route of the bridging ligands BL¹⁻³ and the complexes 1-3.



The ligands were polyaromatic bridging ligands containing two equivalent chelating sites of phenanthroline ring. In the ligands, the two phenanthroline moieties were bridged by a flexible alkoxyphenyl spacer moiety. They were

characterized by IR, ^1H NMR and elemental analysis. In the ^1H NMR spectrum of **BL**¹ (in Fig.1), the signal of Schiff base at 8.64 ppm disappeared and at 4.71 ppm a new weak signal appeared, which indicated the $-\text{C}=\text{N}$ of **L**¹⁻³ were reduced into $-\text{CH}_2-\text{NH}$. The resonances at 9.19, 8.90, 8.27, 7.99, 7.61, 7.47 and 6.75 ppm were assigned to the H_9 , H_2 , H_7 , H_4 , H_8 , H_3 and H_6 protons, respectively, of the phenanthroline ring. The resonances at 7.41 and 6.99 ppm were assigned to the H_{13} and H_{14} protons, respectively, of the phenyl spacer. The H_{15} (methylene) protons of the linker moiety resonate at 4.37 ppm. The H_{12} protons of the methylene resonate at 4.52 ppm and the NH proton at 4.71 ppm. The resonances of **BL**² and **BL**³ were analogous to **BL**¹, and the detailed ^1H NMR information of **BL**² and **BL**³ were shown in the Supporting Information Fig. 3, all ^1H NMR data indicated that $-\text{C}=\text{N}$ were reduced to $-\text{CH}_2-\text{NH}$.

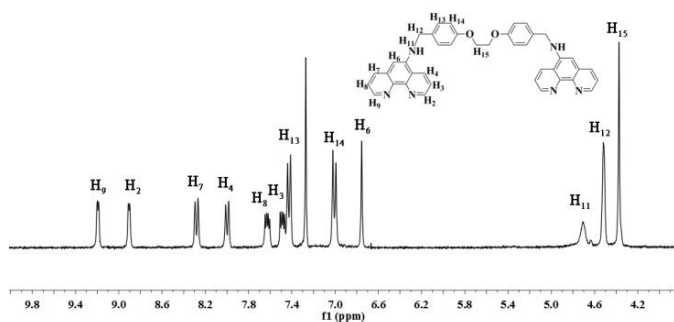


Fig.1 ^1H NMR of **BL**¹ in the CDCl_3

3.2 Synthesis and characterization of Ruthenium complexes 1-3

The dinuclear complexes **1-3** were prepared by the reaction of the preformed double-N, N-bidentate bridging ligands **BL**¹⁻³ with

$\text{Ru}(\text{bpy})_2\text{Cl}_2 \cdot 2\text{H}_2\text{O}$ in ethanol. The complexes were isolated as hexafluorophosphate salt and stable in air and in solution. The elemental analyses suggested the formation of the dinuclear ruthenium complexes. ^1H NMR spectra of complexes **1-3** were recorded in d_6 -DMSO, since the electronic environments of many aromatic hydrogen atoms were very similar, their signals may appear in a narrow chemical shift range (7.2-9.0 ppm). In fact, the aromatic regions of the spectra were complicated, however, the number of the aromatic proton signals were consistent with the number of protons of molecular formula. The partial overlapping of the signals made it difficult to assign all the individual signals respectively. The detailed ^1H NMR information of complexes **1-3** were shown in the Supporting Information Fig. 4. The structures of dinuclear complexes were further established by electrospray mass spectrometry (ESI-MS) in $\text{DMSO}-\text{CH}_3\text{OH}$. This technique has proven to be very helpful for identifying polynuclear metal complexes with high molecular masses. In the ESI-MS of the complex **1**, the peak at m/z 363.7 was due to the dinuclear species **1**⁴⁺; in the ESI-MS of the complex **2**, the peak at m/z 367.2 was due to the species **2**⁴⁺; in the ESI-MS of the complex **3**, the peaks at m/z 887.2, 542.3 and 371.2 were due to the species **[3'2PF₆]²⁺**, **[3'PF₆]³⁺** and **3**⁴⁺, respectively (See Supporting Information Fig. 5). All of these information indicates that the dinuclear ruthenium complexes are stable in the solution.

3.3 Electronic absorption spectra studies

The electronic absorption spectral data of the dinuclear complexes **1-3** were presented in Table 1. The complexes exhibited intense absorption bands at 286 and 360 nm due to the spin-allowed ligand centered (1LC) $\pi-\pi^*$ transition of the ligand framework and a broad band at 460 nm ($\epsilon/\text{dm}^3\text{mol}^{-1}\text{cm}^{-1}$ 26070), 461nm ($\epsilon/\text{dm}^3\text{mol}^{-1}\text{cm}^{-1}$ 22720) and 464 nm ($\epsilon/\text{dm}^3\text{mol}^{-1}\text{cm}^{-1}$ 45470), respectively, assignable to the spin-allowed 1MLCT ($d_\pi-\pi^*$) transition.²³ The MLCT band of the complexes **1-3** with bpy as ancillary ligands were bathochromically shifted with respect to

that of $[\text{Ru}(\text{bpy})_3]^{2+}$ ($\lambda_{\text{max}} = 451 \text{ nm}$) which can be attributed to the extended structural framework of the bridging ligands.²⁴ The Ru(II) complexes were dark red in solution and in the solid state due to the strong 1MLCT absorption band at 460 nm.

3.4 Luminescence spectra studies

The emission spectral data (wavelength of excitation and emission) were presented in Table 1. All measurements were made with solutions deoxygenated by purging argon. The excitation spectra of the complexes **1-3** were monitored at

Table 1 Photophysical and electrochemical data of the complexes **1-3**

complex	Absorption $\lambda_{\text{max}}(\text{nm})$ $\epsilon/10^5\text{dm}^3\text{mol}^{-1}\text{cm}^{-1}$	Excitation $\lambda_{\text{ex}}(\text{nm})$	Emission $\lambda_{\text{em}}(\text{nm})$	$E_{1/2}(\text{V})$	
				Metal centered oxidation	Ligand centered reductions
1	286(1.4), 362(0.2) 460(0.26)	468	601	0.92, 1.37	-0.81, -1.60 -1.86
2	286(1.3), 360(0.2) 461(0.23)	467	602	0.94, 1.42	-0.47, -1.62 -1.83
3	286(2.4), 353(0.4) 464(0.45)	468	602	0.95, 1.44	-0.52, -1.57 -1.81

emission maxima of each complex at room temperature. The excitation spectrum of the free ligands **BL**¹⁻³ contained bands at 286, 302 and 343 nm. The free ligands emitted at 426 nm upon excitation onto the excitation maxima. This fluorescence band of the ligand was no longer observed in its metal complex. The excitation spectrum of complex **1** contained two weak bands at 268 and 373 nm and one intense band at 468 nm, the excitation spectrum of complex **2** contained two weak bands at 267 and 372 nm and one intense band at 467 nm, while the

excitation spectrum of complex **3** contained two weak bands at 264 and 372 nm and one intense band at 468 nm. The complexes **1-3** upon excitation onto their excitation maxima exhibited an emission band at 601, 602 and 602 nm, respectively. The emission profile and emission maxima were similar and independent of the excitation wavelength. The electronic emission spectral of the complexes **1-3** were presented in Fig. 2.

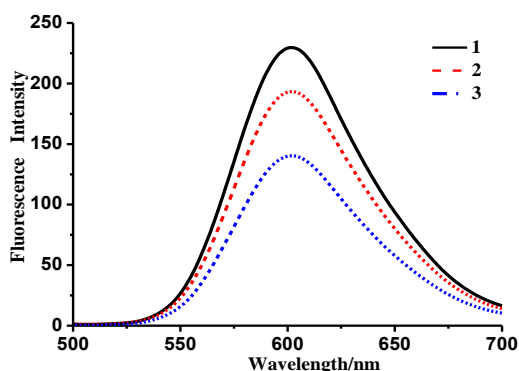


Fig. 2 The emission spectrum of complexes **1-3** in acetonitrile ($1.0 \times 10^{-5} \text{ mol L}^{-1}$, $\lambda_{\text{ex}} = 465 \text{ nm}$)

3.5 Electrochemistry studies

The redox behavior of the complexes **1-3** has been investigated in acetonitrile solution to complement the spectroscopic data. The investigation of electrochemical behavior was very useful to determine the extent of electronic interaction between the metal centers. The cyclic voltammetric data of the complexes were presented in Table 1, and a representative was shown in Fig. 3. All the three complexes exhibited two oxidations in the range of 0-1.5 V. Since the bridging ligands did not exhibit any obvious peaks at the range of 0-1.5 V under the same condition, these peaks of the complexes were all assigned to the redox of the Ru^{II} moieties. In Fig. 3, the oxidations at 0.92 and 1.37 V of complex **1** correspond to the couples $\text{1}^{5+}/\text{1}^{4+}$ and $\text{1}^{6+}/\text{1}^{5+}$, respectively. Oxidation of these complexes stabilized the metal d_{π} -orbital directly and the ligand π^* -orbital indirectly through charge interactions. Subsequent d_{π} - π^* back bonding further stabilized the metal d_{π} -orbital but destabilized the ligand π^* -orbital.²⁵ On reduction, several ill-behaved processes took

place and adsorption of the complexes on the electrode surface also occurred. However, the first reduction potential was still safely measured which was assigned to the reduction of the bridging ligands although more precise assignment could not be made. The first reduction, usually expected to involve the ligand having the most stable lowest unoccupied molecular orbital (LUMO),²⁶ the other two successive reductions were characteristic of the bpy ligands.²⁷ It was concluded that reduction of the complexes occurred first on the bridging ligands and then on the bpy ligands.

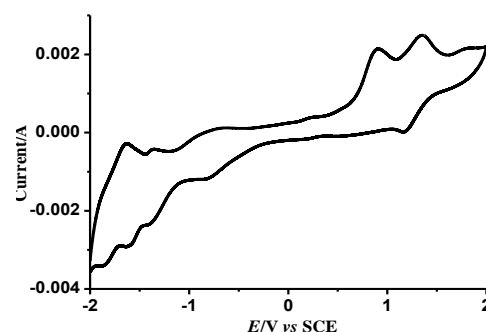


Fig. 3 Cyclic voltammograms (scan rate 100 mV/s) of complex **1**

3.6 Cytotoxicity studies

The cytotoxicity of the complexes **1-3** in vitro were assessed using the method of MTT reduction, culture medium was used as a positive control. After treatment of three cell lines for 48h with complexes **1-3** in a range of concentrations (0.39 - $100 \mu\text{mol L}^{-1}$), the percentage inhibition of growth of the cancer cells was determined. The cell viabilities (%) vs concentrations obtained with continuous exposure for 48 h were depicted in Fig. 4, the IC_{50} values were listed in Table 2.

Table 2 The IC₅₀ of the complexes **1-3**

Complex	IC ₅₀ (μmol L ⁻¹)		
	Hela	SGC-7901	BGC823
1	18.39	21.60	16.14
2	16.04	15.86	13.83
3	13.09	10.38	9.21

The cytotoxicity of the complexes were found to be concentration dependent. The cell viability decreased with increasing concentrations of both complexes. From Table 2, it is clear that complex **3** is generally the most active and exhibits low IC₅₀ values of 9.21 and 10.38 μM for BGC823 and SGC-7901 cells, and complex **1** is less active than complex **2** in three cell lines. The cytotoxicity of complex **3** toward Hela cells is higher than that of [(bpy)₂Ru(L)Ru(bpy)₂]Cl₄ (L=1,6-bis(3-(1Himidazo[4,5-f][1,10]phenanthrolin-2-yl)-9H-carbazol-9-yl)hexane) (IC₅₀ >100 μM).²⁸ The difference in cytotoxicity of these complexes toward the Hela, SGC823 and SGC-7901 cell lines may be caused by different number of methylene groups in the flexible alkane chain. The in vitro activity of anticancer drugs can often be related in part to their lipophilic character, the resulting hydrophobicity may contribute to an increased uptake of the complex by the cells, thereby enhancing the antiproliferative activity.²⁹⁻³³ Alternatively, due to the higher negative mitochondrial membrane potential present in cancer cells, lipophilic cations may preferentially cross the membrane and accumulate in mitochondria,³⁴ thereby leading to the observed higher uptake in cancer

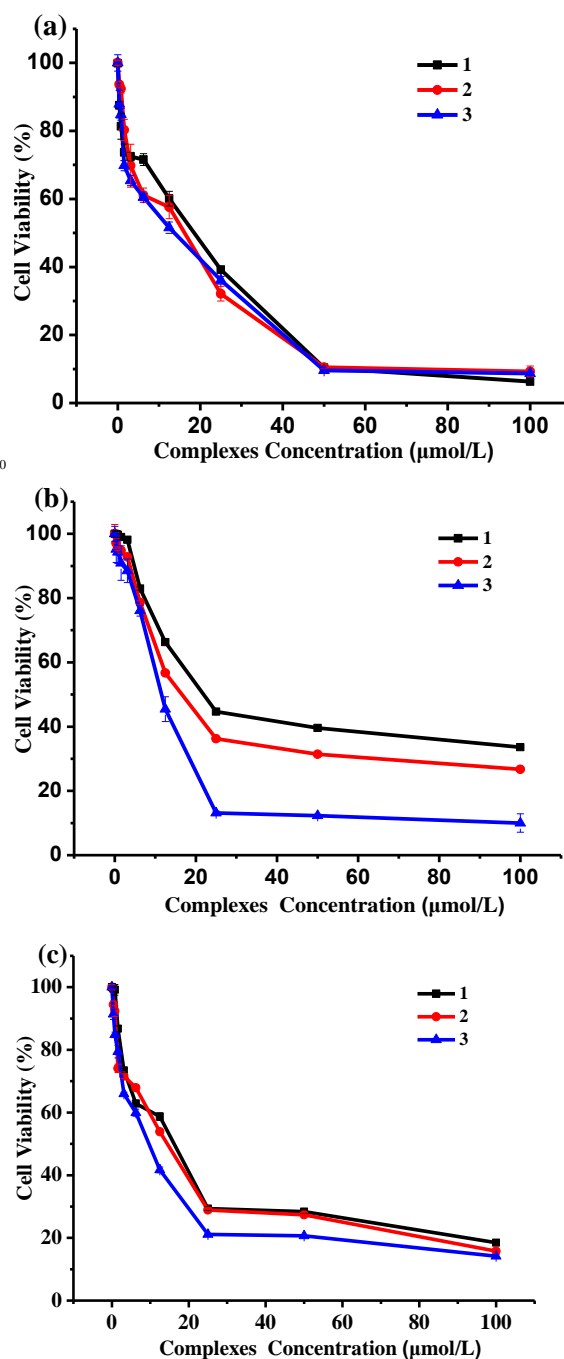
cells.³⁵

Fig.4 Cell viability of complexes **1-3** toward proliferation of Hela (a), SGC-7901 (b) and BGC823 (c) cells in vitro.

3.7 DNA binding studies

The fluorescence measurement was performed to clarify the interaction mode between the complexes and DNA, CT-DNA was chosen as a representative. Complexes **1-3** emit luminescence in a buffer 10 mM Tris and 50 mM NaCl, with a maximum wavelength of about 600 nm when excited at 465 nm. The emission spectra of complexes with the increase in amount of CT-DNA are shown in Fig. 5. The observed luminescence quenching of complexes by CT-DNA is consistent with a photoelectron transfer from guanine base of DNA to the excited MLCT state of the Ru(II) complex as reported in the cases of $[\text{Ru}(\text{bzimpy})_2]^{2+}$, $[\text{Ru}(\text{TAP})_3]^{2+}$ and $[\text{Ru}(\text{bpz})_3]^{2+}$.³⁶⁻³⁸ In addition, it was found that

the interaction between naproxen and ds-DNA in a groove binding mode cause a strong fluorescence quenching.³⁹ This decrease in emission intensity of complexes also agrees with the findings obtained with other non-intercalators.^{40,41} The quenching constants (K_{SV}) using the Stern-Volmer fluorescence quenching equation,⁴² $F_0/F = 1 + K_{SV}[\text{Q}]$, were obtained 1.34×10^5 , 1.46×10^5 and $2.98 \times 10^5 \text{ mol}^{-1} \text{ L}$ for **1**, **2** and **3**, respectively. DNA binding studies by fluorescence spectroscopic titrations reveal that complex **3** binds more strongly to CT-DNA as compared to complexes **1** and **2**. This result is consistent with cytotoxicity.

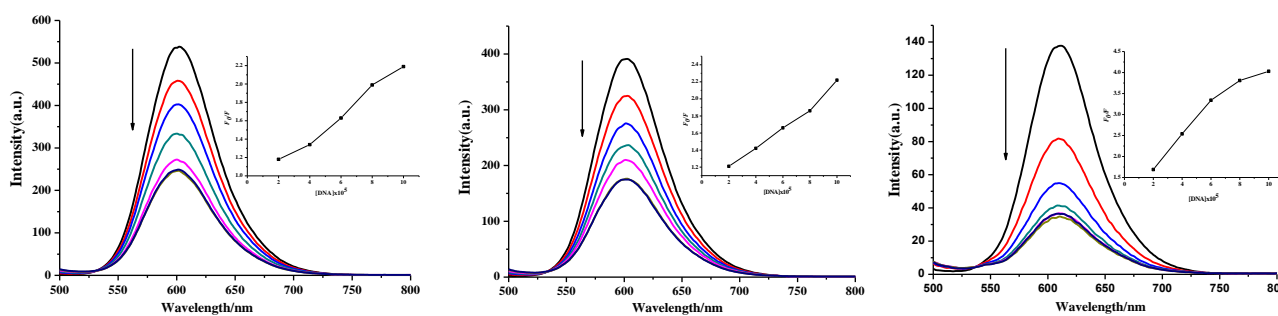


Fig.5 Changes in the fluorescence spectra of complexes **1-3** with increasing concentrations of CT-DNA. Inset: changes of intensity with increasing concentrations of CT-DNA

4. Conclusions

A series of new phenanthroline-based dinucleating bridging ligands and their dinuclear Ru(II) complexes have been synthesized and characterized by elemental analysis, IR, ESI-MS and ^1H NMR techniques. The bridging ligands readily formed dinuclear Ru(II) complexes and their symmetric nature ensured the formation of

dinuclear complexes with equivalent metal centers. Absorption spectra, luminescent properties and electrochemical behavior have been studied and these properties of the Ru(II) species were dominated by MLCT transitions and excited states. The results also showed that each metal-based subunit retained its own spectroscopic properties in the dinuclear arrays.

Cytotoxic assays in vitro of the complexes was studied, according to the studies, Ru(II) complexes showed significant dose-dependent cytotoxicity to cervical cancer(Hela), gastric cancer(SGC-7901) and gastric cancer(BGC823) tumour cell lines, and the more of methylene of bridging ligands, the higher cytotoxicity of the

complexes. The interaction between complexes and CT-DNA were studied using fluorescence spectrometry. The addition of CT-DNA to complexes solution resulted in a strong fluorescence quenching. The interaction between complexes and the CT-DNA may be a groove binding mode.

Acknowledgements

This work was supported by the National Natural Science Foundation of China (No. 21101121), the Natural Science Fund (No. 2010CDB01301) of Hubei Province.

References

- [1] Y. Takeshi, Y. Noguchi, M. Nakai, O. Yamauchi, Y. Nakabayashi, T. Sato, Y. Tamai, M. Chikuma and Y. Mino, *Inorg. Chim. Acta.*, 2013, **394**, 190-195.
- [2] A. Bergamo, A. Masi, P. J. Dyson and G. Sava, *Int. J. Oncol.*, 2008, **33**, 1281-1289.
- [3] A. Bergamo and G. Sava, *Dalton Trans.*, 2007, **13**, 1267-1272.
- [4] A. Levina, A. Mitra and P. A. Lay, *Metallomics*, 2009, **1**, 458-470.
- [5] M. Liu, Z. J. Lim, Y. Y. Gwee, A. Levina and P. A. Lay, *Angew. Chem. Int. Ed.*, 2010, **49**, 1661-1664.
- [6] A. Castonguay, C. Doucet, M. Juhas and D. Maysinger, *J. Med. Chem.*, 2012, **55**, 8799-8806.
- [7] I. Lakomska, M. Fandzloch, T. Muziol, T. Lis and J. Jezierska, *Dalton Trans.*, 2013, **42**, 6219-6226.
- [8] E. Wachter, D. K. Heidary, B. S. Howerton, S. Parkin and E. C. Glazer, *Chem Commun.*, 2012, **48**, 9649-9651.
- [9] A. Grau-Campistany, A. Massaguer, D. Carrion-Salip, F. Barragan, G. Artigas, P. Lopez-Senin, V. Moreno and V. Marchan, *Mol. Pharmaceutics.*, 2013, **10**, 1964-1976.
- [10] R. Pettinari, C. Pettinari, F. Marchetti, C. M. Clavel, R. Scopelliti and P. J. Dyson, *Organometallics*, 2013, **32**, 309-316.
- [11] A. Bergamo, C. Gaiddon, J. H. Schellens, J. H. Beijnen and G. Sava, *J. Inorg. Biochem.*, 2012, **106**, 90-99.
- [12] A. Bergamo, A. Masi, M. A. Jakupiec, B. K. Keppler and G. Sava, *Met-Based Drugs.*, 2009, **2009**, 1-9.
- [13] O. Mazuryk, K. Kurpiewska, K. Lewinski, G. Stochel and M. Brindell, *J. Inorg. Biochem.*, 2012, **116**, 11-18.
- [14] V. Balzani, G. Bergamini, F. Marchioni and P. Ceroni, *Coordin. Chem. Rev.*, 2006, **250**, 1254-1266.
- [15] N. Chanda, R. H. Laye, S. Chakraborty, R. L. Paul, J. C. Jeffery, M. D. Ward and G. K. Lahiri, *J. Chem. Soc., Dalton Trans.*, 2002,

- 18**, 3496-3504.
- [16] V. Balzani, A. Juris, M. Venturi, S. Campagna and S. Serroni, *Chem. Rev.*, 1996, **96**, 759-833.
- [17] J. G. Vos and J. M. Kelly, *Dalton Trans.*, 2006, **41**, 4869-4883.
- [18] J. M. Lehn, *Angew. Chem. Int. Ed.*, 1990, **29**, 1304-1319.
- [19] F. Barigelletti, L. Flamigni, V. Balzani, J. P. Collin, J. P. Sauvage, A. Sour, E. C. Constable and A. M. W. Cargill Thompson, *J. Chem. Soc., Chem. Commun.*, 1993, **11**, 942-944.
- [20] B. P. Sullivan, D. J. Salmon and T. J. Meyer, *Inorg. Chem.*, 1978, **17**, 3334-3341.
- [21] H. B. Donahoe, L. E. Benjamin, L. V. Fennoy and D. Greiff, *J. Org. Chem.*, 1961, **26**, 474-476.
- [22] T. Mosmann, *J. Immunol. Methods.*, 1983, **65**, 55-63.
- [23] A. Bärje, O. Köthe and A. Juris, *J. Chem. Soc., Dalton Trans.*, 2002, **6**, 843-848.
- [24] L. F. Tan, X. H. Liu, H. Chao and L. N. Ji, *J. Inorg. Biochem.*, 2007, **101**, 56-63.
- [25] D. P. Rillema, G. Allen, T. J. Meyer and D. Conrad, *Inorg. Chem.*, 1983, **22**, 1617-1622.
- [26] E. Amouyal, A. Homs, J. C. Chambron and J. P. Sauvage, *J. Chem. Soc., Dalton Trans.*, 1990, **6**, 1841-1845.
- [27] K. Kalyanasundaram, *Coordin. Chem. Rev.*, 1982, **46**, 159-244.
- [28] P. Liu, J. Liu, Y. Q. Zhang, B. Y. Wu and K. Z. Wang, *J. Photoch. Photobio. B.*, 2015, **143**, 89-99.
- [29] M. G. Mendoza-Ferri, C. G. Hartinger, M. A. Mendoza, M. Groessl, A. E. Egger, R. E. Eichinger, J. B. Mangrum, N. P. Farrell, M. Maruszak, P. J. Bednarski, F. Klein, M. A. Jakupiec, A. A. Nazarov, K. Severin and B. K. Keppler, *J. Med. Chem.*, 2009, **52**, 916-925.
- [30] F. Giannini, L. E. H. Paul, J. Furrer, B. Therrien and G. Süss-Fink, *New J. Chem.*, 2013, **37**, 3503-3511.
- [31] Y. Mulyana, D. K. Weber, D. P. Buck, C. A. Motti, J. G. Collins and F. R. Keene, *Dalton Trans.*, 2011, **40**, 1510-1523.
- [32] A. K. Gorle, A. J. Ammit, L. Wallace, F. R. Keene and J. G. Collins, *New J. Chem.*, 2014, **38**, 4049-4059.
- [33] R. J. DeBerardinis, J. J. Lum, G. Hatzivassiliou and C. B. Thompson, *Cell Metab.*, 2008, **7**, 11-20.
- [34] M. P. Murphy, in *Drug-Induced Mitochondrial Dysfunction*, Wiley, Hoboken, 2008, pp. 575-587.
- [35] M. J. Pisani, P. D. Fromm, Y. Mulyana, R. J. Clarke, H. Kerner, K. Heimann, J. G. Collins and F. R. Keene, *ChemMedChem.*, 2011, **6**, 848-858.
- [36] V. G. Vaidyanathan and B. U. Nair, *J. Inorg. Biochem.*, 2002, **91**, 405-412.
- [37] J. M. Kelly, D. J. McConnel, C. Ohuigin, A. B. Tossi, A. K. D. Mesmaeker, A. Masschelein and J. Nasielski, *J. Chem. Soc. Chem. Commun.*, 1987, **1149**, 1821-1823.

- [38] A.K.De-Mesmaeker, G.Orellana, J.K.Barton and N. Turro, *J. Photochem. Photobiol.*, 1990, **52**, 461-472.
- [39] B. F. Ye, Z. J. Zhang and H. X. Ju, *Chin. J. Chem.*, 2005, **23**, 58-62.
- [40] I.H. Bhat and S.Tabassum, *Spectrochim. Acta A.*, 2009, **72**, 1026-1033.
- [41] N. Shahabadi, S. Kashanian and F. Darabi, *Eur.J.Med.Chem.*, 2010, **45**, 4239-4245.
- [42] N. Shahabadi, S. Kashanian and F. Darabi, *DNA Cell Biol.*, 2009, **28**, 589-596.